Int. J. Therm. Sci. (2000) 39, 471–480

S1290-0729(00)00202-7/FLA

Phonon heat conduction in nanostructures [1]

Gang Chen *

Mechanical and Aerospace Engineering Department, University of California, Los Angeles, CA 90095, USA

(Received 11 August 1999, accepted 8 September 1999)

Abstract — Phonon heat conduction mechanisms in nanostructures may differ significantly from those in macrostructures. In this paper, we illustrate the fundamental differences between heat conduction in nanostructures and macrostructures based on examples we have been working on, including particularly heat conduction in superlattices, nanowires, and nanoparticles. The prospects of control heat conduction in nanostructures through phonon engineering are discussed. Examples are given to demonstrate the importance of nanoscale heat transfer in microelectronics and energy technology. © 2000 Éditions scientifiques et médicales Elsevier SAS

phonons / heat conduction / thermal conductivity / phonon engineering / nanostructures / nanoparticles / superlattices / nanowires / thermoelectrics / thermal managements

Nomenclature

C	phonon volumetric specific heat	$J \cdot m^{-3} \cdot K^{-1}$
h	device characteristic length	m
k	thermal conductivity	$W \cdot m^{-1} \cdot K^{-1}$
S	Seebeck coefficient	$V \cdot K^{-1}$
T	temperature	K
v	phonon group velocity	$m \cdot s^{-1}$
Z	thermoelectric figure of merit	K^{-1}
Λ	phonon mean free path	m
σ	electrical conductivity	$\Omega^{-1} \cdot m^{-1}$
ω	phonon angular frequency	Hz

1. INTRODUCTION

Driven by the interweaving curiosity of mankind and the microelectronics industry, miniaturization hallmarks the science and technology of the last few decades of this century. Advanced fabrication technology now makes it routine to fabricate submicron devices and grow atomic layer of thin films, which allow the realization of scientific dreams as to engineer the electronic and optical properties based on size effects. Large amount of work has been done and is still going strong in these areas, which have lead to many novel and improved devices such as quantum-well semiconductor lasers. In contrast, little attention has been devoted to the study of phonon heat conduction in nanostructures. Although microscale heat transfer has drawn significant attention in the heat transfer community during the past decade, many fundamentally as well as practically significant questions await to be answered and their impact to the microelectronics and the energy technologies remain to be explored [1].

Phonon heat transfer at the nanoscale differs from that at the macroscale due to several fundamental reasons [2, 3]. In bulk materials, internal scattering dominates the heat transfer processes. As the size shrinks, the frequency of the phonon–boundary collision increases, and so does the surface/interface to the volume ratio. The interface scattering of phonons and the associated thermal boundary resistance can dominate heat conduction in nanostructures. The size effects, however, are not limited to the thermal processes inside nanostructures. In the vicinity of small devices, phonons become rarefied when their mean-free-path is comparable or larger than the device size, which effectively increases the thermal resistance for removing heat from the devices. In addition, the phonon spectra can also be altered in small structures. Understanding these physical processes is important not only for the prediction of the microelectronic device tem-

* gchen@seas.ucla.edu

[1] Based on a paper presented as a plenary talk at Eurotherm Seminar No. 57 "Microscale Heat Transfer", Poitiers, France, July 8–10, 1998.

perature rise and reliability, but also can enable new technology development such as low dimensional thermoelectrics [4, 5].

In this paper, we will explain some of the fundamental differences between phonon heat conduction at the nanoscale and macroscale, and illustrate the implications of the new knowledge we learnt on microelectronics and thermoelectrics. We will start from a discussion of the phonon characteristic lengths and the different transport regimes. Examples will be given in the following sections to illustrate the transport phenomena in different regimes and the transition among different regimes. The prospects of engineering phonon transport will be discussed, in association with their applications in microelectronics and low-dimensional thermoelectrics.

2. PHONON MEAN FREE PATH AND COHERENCE LENGTH

Phonons are the quantized lattice vibrations and they are the major heat carriers in semiconductors as well as in dielectrics. Although phonon is inherently a wave concept, the coherence length of thermal phonons is short and for heat conduction, it is more convenient to treat phonons as particles. Based on the kinetic theory, the mean-free-path (MFP), Λ, of phonons in a material can be related to its thermal conductivity, k, through

$$k = \frac{C v \Lambda}{3} \tag{1}$$

where C is the specific heat per unit volume and v is the speed of sound. The phonon MFP is determined by various scattering mechanisms inside the medium, including phonon–phonon scattering due to the anharmonic force interaction, phonon–impurity scattering, and phonon–boundary scattering [6, 7]. In using the above relation to estimate the phonon MFP, it should be kept in mind that equation (1) is derived under the assumption that all phonons have the same energy and velocity. In real crystals, the picture differs significantly from this assumption because of the phonon dispersion. Considering the frequency dependence of the phonon group velocity, scattering rate, and the specific heat, the thermal conductivity can be expressed as [6, 7]

$$k = \frac{1}{3} \sum_p \int C(\omega) v(\omega) \Lambda(\omega) \, \mathrm{d}\omega \tag{2}$$

where the summation is over different phonon branches, and the integration is over the phonon spectrum width of each branch. Typically, the contribution of optical phonons to the thermal conductivity is small due to their small group velocity. A more realistic approximate estimation of the phonon MFP can be obtained from considering the frequency dependence of the phonon specific heat and phonon group velocity [8, 9]. *Table I* compares the phonon MFP estimated from equations (1) and (2) for several typical materials [9, 10]. The much longer phonon MFP obtained from equation (2) arises from the following two factors: (1) the group velocity of acoustic phonons depends strongly on their frequency; at the zone boundary where the phonon specific heat is large, their group velocity is small compared to that at the zone center; and (2) optical phonons generally have very small group velocities throughout the Brillouin zone; their contribution to thermal conductivity was neglected.

The phonon coherence length [9] is a less used concept but can be readily understood by making an analogy to the photon coherence length in optics [11]. The coherence length determines whether the interference effect associated with a wave can be observed or not, and thus whether the modeling of heat conduction should

TABLE I
Room temperature phonon properties calculated from equations (1) (called the Debye model) and (2) (called the dispersion model) [9, 10].

Material	Model	Specific heat, $\cdot 10^6$ J·m^{-3}·K^{-1}	Group velocity, m·s^{-1}	Mean-free-path, Å
GaAs	Debye	1.71	3 700	208
	Dispersion	0.88	1 024	1 453
AlAs	Debye	1.58	4 430	377
	Dispersion	0.88	1 264	2 364
Si	Debye	1.66	6 400	409
	Dispersion	0.93	1 804	2 604
Ge	Debye	1.67	3 900	275
	Dispersion	0.87	1 042	1 986

start from the phonon wave picture or can simply treat phonons as particles. The coherence length depends on the spectral width of the source, the medium that the wave goes through, and the bandwidth of the detector. One example is the transmission of radiation through a thin film [12]. Although the transmissivity of a monochromatic wave through a film always shows an interference phenomenon, whether or not one can observe the interference phenomenon for a polychromatic incident wave depends on the film thickness, structure, and the detector bandwidth. For a thick film with a wide band detector, the interference phenomenon cannot be resolved due to the random superposition of the interference peaks and valleys among all the wave components constituting the polychromatic source. As a consequence, geometrical optics, i.e., ray tracing, can be used to calculate the transmissivity of the film. For heat conduction by phonons, both the heat source (thermally excited phonons) and the detector (i.e., temperature sensor) cover a wide band spectrum of the phonons. The coherence length is thus expected to be short. An estimation of the phonon coherence length in bulk GaAs is shown in *figure 1* [9]. At room temperature, the coherence length is only of the order of 10–20 Å, much smaller than the phonon MFP.

In the study of the transport properties and thermal modeling of microdevices, a critical question is what are the pertinent basic equations to start from. For the thermal modeling of macrostructures, the Fourier heat conduction theory is often the starting point. When the device size becomes comparable or smaller than the MFP or the coherence length, however, the validity of the Fourier heat conduction theory is questionable

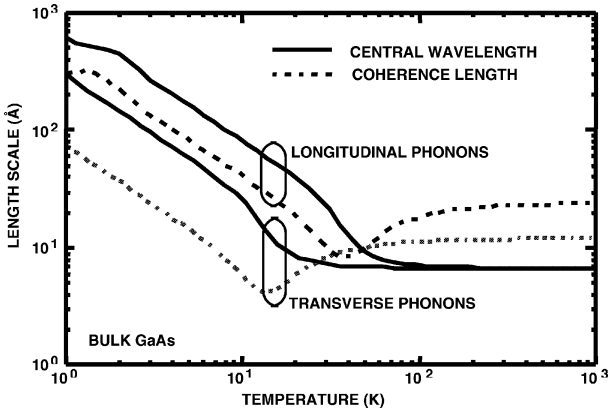

Figure 1. Coherence length and central wavelength in bulk GaAs [9].

and more fundamental and microscopic theories may have to be applied [1–3]. While not many studies have been carried out for phonon transport in nanostructures, analogy can often be made between phonon transport and that of electrons and photons, for which large amount of literature can be found [2]. *Table II* illustrates different transport regimes for these common energy carriers, including typical values of various characteristic lengths at room temperature. Examples will be given in the following two sections to illustrate transport phenomena in and transition between different regimes.

3. PHONON WAVE HEAT CONDUCTION

Most of the wave characteristics of phonons can be obtained from the wave equations established under New-

TABLE II
Transport regimes for three common energy carriers[2].

Length scale	Regimes	Photon	Electron	Phonon
Wave regime coherence length, L	$h < \mathrm{O}(L)$ wave	Maxwell EM theory	quantum mechanics	quantum mechanics
photon: 1 μm–1 km electron: 10–1000 Å phonon: ∼20 Å	$h \sim \mathrm{O}(L)$ partial coherence	optical coherence theory	electron coherence theory	phonon coherence theory
Particle regime mean free path, Λ	$h < \mathrm{O}(\Lambda)$ ballistic	ray tracing	ballistic transport	ray tracing
photon: ∼100 Å–1 km electron: ∼300 Å	$h \sim \mathrm{O}(\Lambda)$ quasi-diffusive	radiative transfer equation	Boltzmann transport equation	Boltzmann transport equation
phonon: ∼300 Å	$h > \mathrm{O}(\Lambda)$ diffusive	diffusion approximation	Ohm's and Fourier's laws	Fourier's law

[2] Device characteristic length (such as thickness) is h; O denotes the order-of-magnitude; the listed MFP and coherence lengths are typical values but these values are strongly material and temperature dependent.

ton's second law [13, 14]. Under the harmonic oscillator approximation, a quantum mechanical treatment of lattice waves normally does not invalidate results of the classical approach, such as the phonon dispersion and the density of states, but leads to the additional result that the energy of a quantum mechanical state equals the product of an integer and a minimum energy (plus a zero-point energy). This minimum quantum of energy is called a phonon. Neither does the concept of phonon is invalidated by nanostructures due to the small number of atoms, because the vibration of a cluster of atoms can always be decomposed into the superposition of waves by the Fourier series. The relationship between the wavelength and frequency obtained from such a decomposition gives the phonon dispersion relation, as commonly used for bulk materials. However, when the number of atoms are small such that the individual atoms can be traced as a function of time and space, it is questionable whether phonon is a worthwhile concept because direct molecular dynamics simulation may answer the heat transfer problem better.

In nanostructures, phonon waves are frequently scattered at surfaces and interfaces. The scattered wave may interfere with the incoming waves, thus altering the phonon dispersion. This alteration in turn affects the phonon density of states, group velocity, scattering mechanisms, and the specific heat, leading to a change of the apparent thermal conductivity of nanostructures.

There are several ways to treat phonon wave heat conduction in nanostructures. The first is based on treating phonons as classical acoustic waves with quantum corrections. As an example, *figure 2* gives the effective phonon thermal conductivity across a Ge/Si/Ge-like double heterojunction structure [15]. The wave results are obtained from calculating the acoustic wave propagation in thin film structures and integrating over all phonon propagating directions and allowable energy levels, while neglecting the internal scattering of phonons. Accompanying the wave model results is the thermal conductivity of the thin film obtained by treating phonons as particles. A comparison of the wave and the particle model results indicate that phonon wave effects are not significant at room temperature unless films are less than 10 Å in thickness. Below 10 Å, tunneling of phonon waves above the critical angles increases the effective thermal conductivity across the film.

In the acoustic wave approach, it is difficult to treat the internal phonon scattering processes. Another way to consider the phonon wave effect is based on first solving the Schrödinger equation or the classical equation of motion to obtain the phonon dispersion relation of nanostructures by assuming harmonic force interaction among atoms. The effective thermal conductivity of the structure is obtained subsequently from solving the Boltzmann transport equation, as is typically done for the bulk-material thermal conductivity modeling [6, 7]. The wave interference and tunneling phonomena [15] are included through the changes in the density of states, the phonon group velocity, and the scattering mechanisms. Calculations of the phonon normal modes in superlattices and nanostructures have been carried out based on the classical lattice dynamics theory [16, 17] or quantum mechanics [18, 19]. Hyldgaard and Mahan [20] evaluated the cross-plane thermal conductivity of superlattices based on the change of the phonon dispersion on the group velocity and the density of states in superlattices structures. Their results indicate that the thermal conductivity in Si/Ge superlattices can be reduced by an order of magnitude. It should be pointed out, however, that similar conclusions can be obtained by treating the phonons as particles [10, 21]. The detailed heat conduction mechanisms are not fully understood at this stage, as will be discussed later.

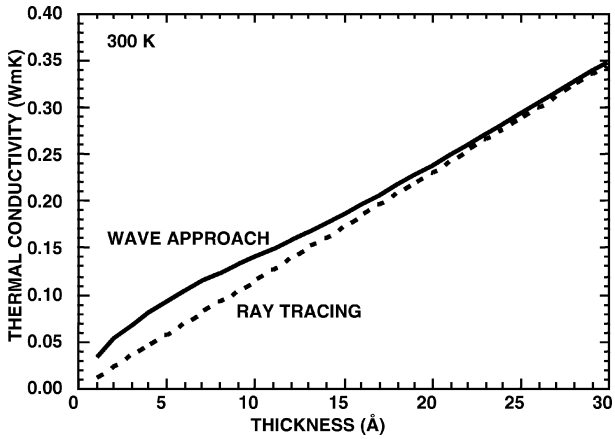

Figure 2. Thermal conductivity of a double heterojunction structure due to transverse phonons as a function of the film thickness, using models based on (1) the particle and (2) the wave approaches, demonstrating that the two approaches give similar results because of the short phonon coherence length [15].

A direct method that may include both the wave effects and the internal scattering is the molecular dynamics (MD). *Figure 3* shows the MD simulation of the thermal conductivity of Si nanowires [22], demonstrating a significant reduction on the thermal conductivity of such wires. The limitation of the MD method, however, is the computational power and the accuracy of the interatomic potential. Embedded in the MD results are the physics of the phonon heat conduction processes. It is not a trivial task to understand the physics behind the MD results.

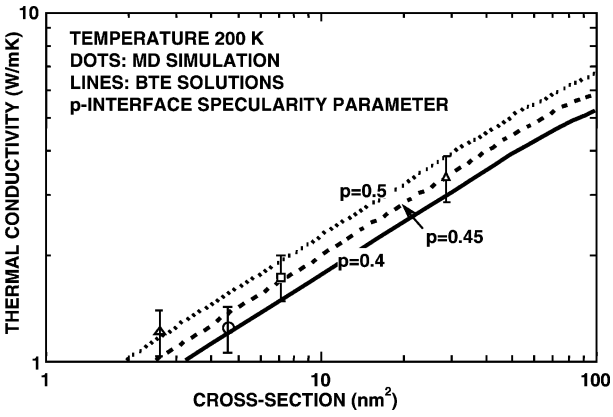

Figure 3. Thermal conductivity of square silicon nanowires based on molecular dynamics simulation and the Boltzmann transport equation solution [22].

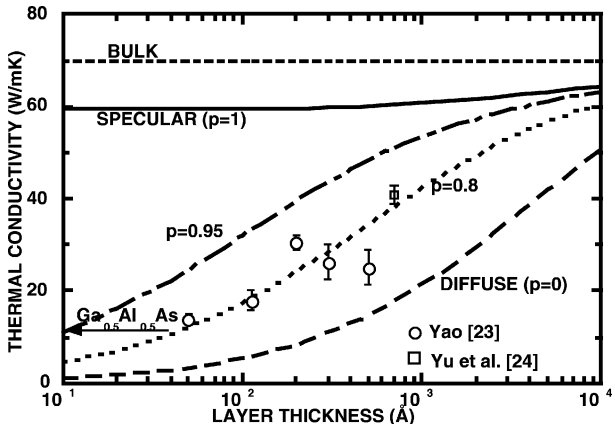

Figure 4. Modeled [9] and measured [23, 24] in-plane thermal conductivity of GaAs/AlAs superlattices as a function of the layer thickness. The specularity parameter p represents the fraction of specularly scattered phonons at the interface [9].

4. CLASSICAL SIZE EFFECTS

As the device characteristic length becomes much longer than the coherence length, the wave effects are negligible and phonons can be treated as particles. In this classical regime, size effects can be manifested for transport inside nanostructures, across the interfaces, and outside nanostructures.

4.1. Transport inside nanostructures

As the size of a nanostructure becomes comparable or smaller than the phonon MFP, phonons collide with the boundary more often than in bulk materials. This additional collision mechanism increases the resistance to heat flow and thus reduces the effective thermal conductivity of thin films and wires. *Figure 4* shows modeling [9] and experimental [23, 24] results on the in-plane thermal conductivity of GaAs/AlAs superlattices based on solving the Boltzmann transport equation. The model includes the frequency dependence of the scattering time and the group velocity. It is based on the assumption that interfaces scatter phonons partially diffusely and partially specularly, as represented by the specularity parameter p, which vanishes in the purely diffuse limit and approaches unity for totally specular reflection/transmission at interfaces. This figure suggests that the in-plane thermal conductivity of superlattices depends strongly on how interfaces scatter phonons as well as on the thickness of the layers. If phonons are specularly scattered at the interface, the thermal conductivity of the superlattices is close to their bulk value, i.e., the value calculated from the Fourier heat conduction theory based on the bulk material properties. In this case, interfaces behave like a wave guide. With a slight presence of diffuse phonon scattering at interfaces, however, the thermal conductivity of superlattice structures drops sharply. By engineering the interface structures appropriately, it may be possible to control the thermal conductivity. The sensitivity of the thin film thermal conductivity to the interface scattering process depends strongly on the film thickness. The thinner the film, the more sensitive is the thermal conductivity to the diffuse scattering at the interface. For microelectronics, a large thermal conductivity is often desirable to channel out the heat dissipated inside the device. For the Bragg reflector used in vertical cavity surface emitting lasers, for example, the layer thickness should be maintained as large as possible to avoid the penalty on device temperature rise due to the reduction of the thermal conductivity [25]. For thermoelectric devices, low thermal conductivity is necessary. *Figure 4* suggests that the superlattice thermal conductivity can be reduced even below that of their corresponding alloy, while alloying has been a standard method used to reduce the thermal conductivity in bulk materials for thermoelectric applications [26]. The alloying of semiconductor constituents, however, also lowers the electron mobility and conductivity.

The above discussion focuses on phonon transport in thin films. It is not difficult to understand that similar but stronger size effects will occur inside one-dimensional (quantum wires) and zero-dimensional (quantum dots) structures. *Figure 5* compares the estimated thermal conductivity of Si thin films and wires, together with some reported experimental data on the thermal conductivity of single crystal Si thin films [27–29]. The thermal con-

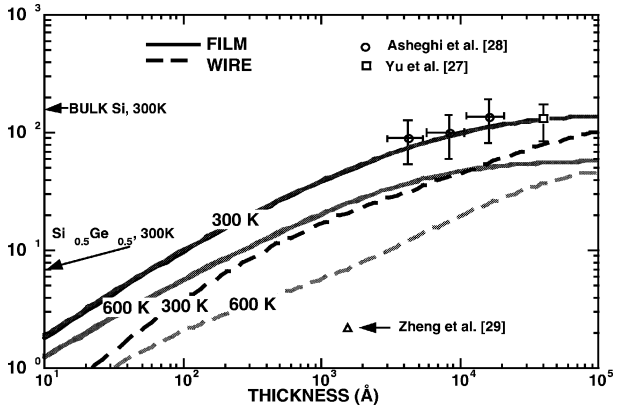

Figure 5. Estimated thermal conductivity of Si films and wires as a function of the film thickness and wire diameter. Experimental data points are for Si films [27–29].

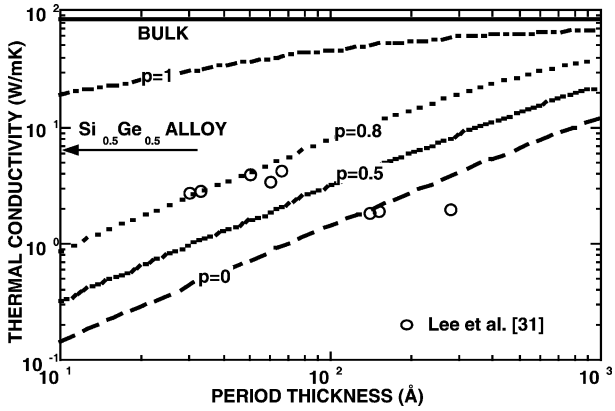

Figure 6. Effective thermal conductivity of Si/Ge superlattices in the cross-plane direction, model [10] and experiment [31].

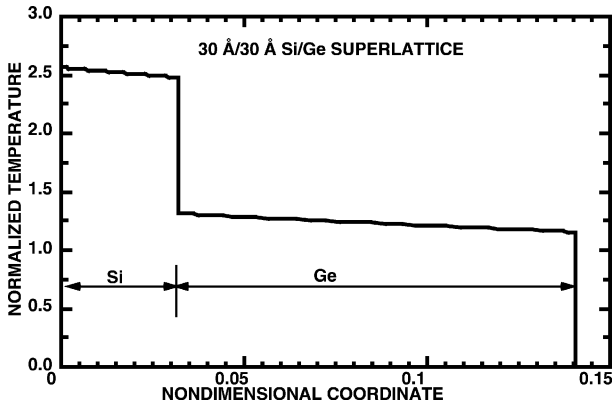

Figure 7. Temperature distribution in one period of a Si/Ge superlattice by assuming diffuse ($p = 0$) interface phonon scattering. The coordinate in each layer is normalized to the phonon MFP in the layer. This figure demonstrates that most of the temperature drops occur at the interface. Phonon transport inside the film is ballistic [10, 21].

ductivity of wires drops faster with thickness as a result of increased phonon scattering in the direction perpendicular to the wire axis.

4.2. Thermal boundary resistance

When heat flows in the direction perpendicular to the interface of two materials, a temperature drop may develop even if the interface is atomically flat because of the mismatch in the phonon velocity and density of the two materials. This phenomenon, called the thermal boundary resistance [30], becomes more important as the number of device layers increases in microelectronic devices. Interface thermal boundary resistance can dominates the thermal conductivity of superlattice structures. *Figure 6* shows an example of the modeling [10, 21] and the experimental results on the cross-plane thermal conductivity of Si/Ge superlattices [31]. The temperature drop across one period of a superlattice is given in *figure 7*. In this case, the phonon transport inside each layer is totally ballistic, thus only a very small fraction of the total temperature drop occurs inside the film. The majority of the temperature drop develops at the interfaces. The effective thermal conductivity of the structure has almost no direct relation to the thermal conductivity of the bulk materials making up the film but depends almost entirely on the mismatches of the phonon velocity, specific heat, and density between the two media. As an example, the thermal conductivity of a $\sim$70 Å period Si/Ge superlattices is $\sim$4.5 $\mathrm{W{\cdot}m^{-1}{\cdot}K^{-1}}$, smaller than that of comparable GaAs/AlAs superlattices, $\sim$6 $\mathrm{W{\cdot}m^{-1}{\cdot}K^{-1}}$ [32], because larger mismatches in the above properties exist between Si and Ge than between GaAs and AlAs. The Fourier heat conduction theory would predict an effective thermal conductivity of 85 $\mathrm{W{\cdot}m^{-1}{\cdot}K^{-1}}$ for Si/Ge superlattices of equal layer thickness and 60 $\mathrm{W{\cdot}m^{-1}{\cdot}K^{-1}}$ for similar GaAs/AlAs superlattices, which are not only an order of magnitude larger but also opposite to the trend of experimental observation. To further demonstrate this point, we have measured the thermal conductivity of Si(50 Å)/$\mathrm{Si_{0.69}Ge_{0.31}}$(10 Å) superlattices [33]. The cross-plane thermal conductivity of this structure is 11.1 $\mathrm{W{\cdot}m^{-1}{\cdot}K^{-1}}$, while the effective thermal conductivity of such a structure from the Fourier heat conduction theory is 39.8 $\mathrm{W{\cdot}m^{-1}{\cdot}K^{-1}}$. In contrast, the thermal conductivity of a pure Si(48 Å)/Ge(12 Å) superlattice is reported to be 3 $\mathrm{W{\cdot}m^{-1}{\cdot}K^{-1}}$ [31] compared to an effective value of 115 $\mathrm{W{\cdot}m^{-1}{\cdot}K^{-1}}$ obtained from the Fourier theory for this structure. The smaller thermal conductivity

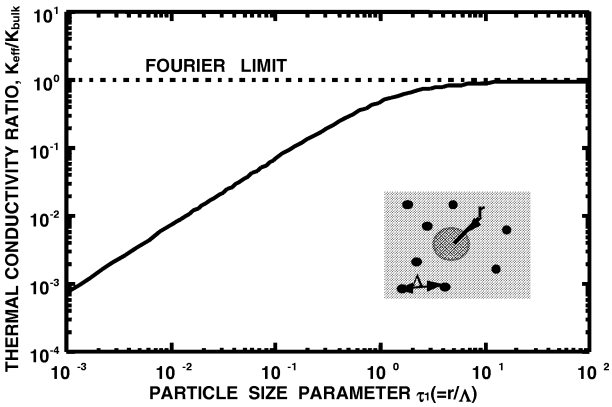

Figure 8. Rarefied phonon heat conduction surrounding a small sphere. The effective thermal conductivity that the sphere feels about its surrounding medium is reduced as the sphere radius becomes smaller than the phonon MFP in the surrounding medium [34].

reduction in the Si/SiGe is due to the smaller mismatch in the phonon properties between Si and $Si_{0.69}Ge_{0.31}$ alloy. This suggests that it is possible to engineer the worst thermal conductors from a composite of the best thermal conductors, such as diamond, by mating it with another material which has a large mismatch in velocity, specific heat, and density relative to diamond. One condition when taking such an approach is that the film thickness must be smaller than the phonon MFP in bulk materials such that the phonon transport inside the film is ballistic and the interface effects become dominant.

4.3. Rarefied phonon gas outside nanostructures

Size effects on phonon transport are not limited to processes occurring inside device structures. They occur in the vicinity of small devices as well. The insert to *figure 8* shows a simple example in which a device embedded inside a substrate is represented by a heat generating sphere. The heat generated inside the device is eventually carried away by phonons in the substrate. When the device radius becomes smaller than the phonon MFP in the substrate, phonons in the substrate become rarefied relative to the device size and, as a consequence, it becomes more difficult for heat to escape from the device. This situation is similar to rarefied gas heat conduction. We have modeled heat conduction surrounding a heat generating sphere [34]. *Figure 8* gives the effect thermal conductivity that the sphere "feels" about the substrate normalized to the bulk thermal conductivity of the substrate. The results of *figure 8* show that the effective thermal conductivity is much smaller than that of the substrate when the sphere radius is smaller than the phonon MFP in the substrate. This translates into a higher temperature for the sphere. As an example, assuming that the sphere generates 1 mW of heat and it is embedded in a Si substrate, its temperature rise is 16 °C when the sphere diameter is 0.25 μm but becomes 160 °C at 70 nm (a room temperature phonon MFP of 2 500 Å in Si is taken in the calculation). If we assume that the power dissipation in the sphere scales linearly with the radius, similar to the power dissipation in a MOSFET device that scales linearly with the channel length, the device temperature in a 70 nm diameter sphere would be 45 °C. This temperature rise is superimposed on the average temperature rise of the substrate, indicating that severe device heating may be encountered due to the rarefied phonon gas effect.

5. PHONON ENGINEERING

The fact that thermal transport properties in nanostructures are affected by the size leads to the possibility of engineering structures towards desired properties for different applications. It has been demonstrated in the last three decades that the electronic and optical properties can be engineered to a high degree of precision in quantum structures, by using quantum size effects on electrons. This is called the bandgap engineering [35]. In the last decade, the idea of control radiative properties also emerged such as the photonic crystals [36]. It is natural to think whether one can control phonons for the desired thermal properties.

Both the bandgap engineering and the photonic crystals are based on the wave properties of either electrons or photons. Compared to electrons and photons, the wavelengths of dominant phonons at room temperature are typically much shorter and so is the coherence length. This may set a limitation regarding to how much one can do in engineering the thermal transport properties based on the wave effects. It should be emphasized, however, that the wave effects remain very much unexplored.

The classical size effects on phonon transport points to other directions of phonon engineering. The previous examples show that the effective thermal conductivities of thin films and wires depend strongly on the interface conditions, and the mismatch of the phonon properties in different layers. We have commented that by engineering the interfaces and the mismatch of the phonon properties in different layers, it may be possible to control the thermophysical properties towards the desired directions

TABLE III
Thermal diffusivity of three different GaAs/AlGaAs structures ($cm^2 \cdot s^{-1}$) [23, 37].

	Parallel direction		Perpendicular direction	
	Bulk	Measured	Bulk	Measured
MBE635[3]	0.23	0.23	0.2	0.13
MBE362[4]	0.33	0.068	0.3	0.026
MBE849[5]	0.41	0.25		

[3] MBE 635 is a two layer structure consisting of 10 μm GaAs and 1 μm $Al_{0.67}Ga_{0.33}As$. The measured thermal diffusivities are close to their bulk values due to the large layer thickness.

[4] MBE362 is made of a GaAs(∼700 Å)/$Al_{0.67}Ga_{0.33}As$(∼700 Å) VCSEL structure in which $Al_{0.67}Ga_{0.33}As$ consists of GaAs/AlAs short period superlattices of comparable atomic composition. The measured thermal diffusivities are much smaller than their corresponding bulk values, demonstrating the strong effect of interfaces on the thermal conductivity.

[5] MBE849 is a pure GaAs/AlAs (700 Å/700 Å) periodic structure. Its thermal diffusivity is larger than MBE362 due to the smaller number of interfaces.

such as to improve the thermal conductivity or to degrade the thermal conductivity. Both of these two directions have significant practical applications. In the following, we will give two examples to illustrate these applications.

5.1. Improving thermal conductivity for microelectronics

The classical size effects discussed so far tend to increase the resistance to phonon heat conduction, which is detrimental for microelectronics and optoelectronic devices. Without changing the materials, the best one could hope to do is to recover the thermal conductivity of thin film systems to the bulk level. In the design of devices, this means that the film thickness should be increased to the maximum allowable value and the number of thin film layers should be reduced to a minimum. As an example, *table III* lists the thermal diffusivity of two periodic structures that we have measured [23, 37]. MBE362 is a vertical-cavity surface-emitting laser (VCSEL) structure that is made of mainly GaAs/$Al_{0.67}Ga_{0.33}As$ quarter wavelength (of the laser light inside the device) layers (∼700 Å each layer). The quarter wavelength $Al_{0.67}Ga_{0.33}As$ layer in this structure is approximated by short period GaAs/AlAs superlattices of a comparable atomic composition during the film growth. MBE849 is a periodic structure of comparable thickness (700 Å each layer) but made of pure GaAs and AlAs layers. The measured thermal diffusivities of the two similar structures, although both are smaller than the values calculated from the Fourier heat conduction theory, are drastically different. MBE849 has a high in-plane thermal conductivity than the MBE362 because the latter has too many interfaces resulting from the short period superlattices. For VCSELs, the reduced thermal conductivity in the device layer alone increases the active region temperature significantly because the heat generation density is high and a large portion of the temperature rise of the device develops inside the device layer. *Figure 9* shows modeling and experimental results on the temperature rise as a function of current for an external-cavity VCSEL structure [25, 38]. The dashed line is obtained by assuming that the thermal conductivity equals the value calculated from the bulk thermal conductivity of the structure. The actual device temperature is clearly increased by the reduced thermal conductivity of the VCSEL structure (similar to MBE362). This example suggests that through concurrent electrical, optical, and thermal consideration at the device level, large gains in the device temperature reduction may be possible.

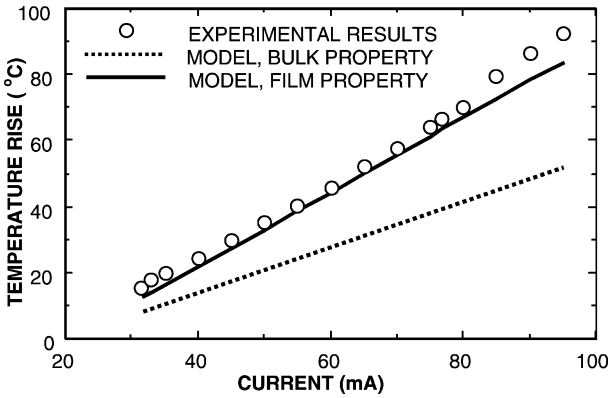

Figure 9. Measured and modeled temperature rise in an external-cavity surface-emitting laser, demonstrating that a large temperature rise inside the device is caused by the reduced thermal conductivity of the mirror [25, 38].

5.2. Reducing thermal conductivity for thermoelectric applications

In the previous example on semiconductor lasers, high thermal conductivity of the device structures is desirable. For energy conversion devices such as solid state thermoelectric [4, 5] and thermionic devices [39, 40], low thermal conductivity materials are often desired to isolate the reverse heat leakage between the hot and the cold junctions. For example, the efficiency of a thermoelectric device is determined by the dimensionless

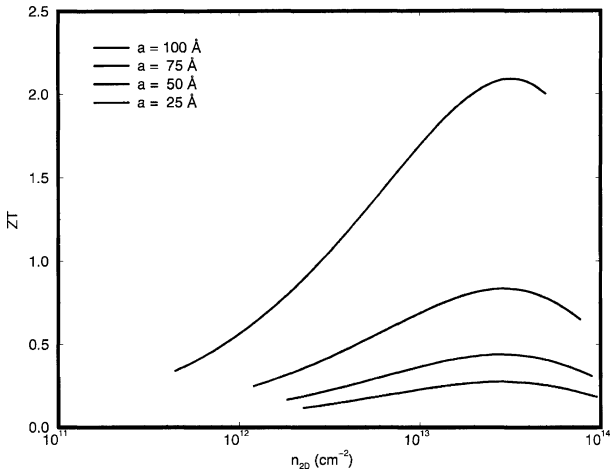

Figure 10. Calculated nondimensional thermoelectric figure of merit (ZT) as a function of the carrier concentration in Si quantum wells for different well widths [41].

thermoelectric figure-of-merit, ZT [26],

$$ZT = \frac{S^2 \sigma T}{k} \tag{3}$$

where S is the Seebeck coefficient, T the absolute temperature, and σ the electrical resistivity. The numerator is called the power factor and it is determined by electron transport properties. The thermal conductivity in the denominator is mainly controlled by phonon transport. Equation (3) suggests that size effects can be used to the advantage of thermoelectric devices to increase ZT. In particular, it has been demonstrated in the last few years that the power factor in low-dimensional structures can be significantly increased above those of their bulk materials [4, 5]. Through concurrent consideration of electron and phonon transport in low-dimensional systems, it should be possible to engineer low-dimensional structures for high ZT. *Figure 10* shows the calculated ZT as a function of the doping concentration of Si quantum wells with different well width based on concurrent modeling the electron and phonon transport in quantum structures [41], indicating a significant increase in ZT could be achieved. A more detailed discussion on the thermal conductivity reduction through phonon engineering is published elsewhere [42].

6. CONCLUDING REMARKS

Phonon heat conduction mechanism in nanostructures may differ significantly from that in macrostructures. Examples of phonon size effects include: increased phonon scattering at the boundaries and interfaces; phonon rarefaction surrounding small structures; and the modification of the phonon dispersion relations. A clear understanding of these effects enables phonon engineering to control the phonon transport processes for different applications. For microelectronics, phonon engineering can provide better structural and device designs to minimize the impacts of adverse size effects on the device temperature rise. For thermoelectrics and thermionics, phonon engineering can be used to reduce the thermal conductivity of thin-film structures to provide better thermal isolation between the heat source and the heat sink.

Acknowledgement

This work was partially supported by an ONR MURI project on low-dimensional thermoelectrics (N0014-97-1-0516) and an NSF young investigator award.

REFERENCES

[1] Tien C.L., Chen G., Challenges in microscale conductive and radiative heat transfer, J. Heat Tran. 116 (1994) 799–807.

[2] Chen G., Micro- and nanoscale heat transfer in photonic devices, in: Tien C.L. (Ed.), Annual Review of Heat Transfer, Vol. 7, 1996, pp. 1–59.

[3] Tien C.L., Majumdar A., Gerner F.M., Microscale Energy Transfer, Taylor and Francis, 1998.

[4] Hicks L.D., Dresselhaus M.S., Effect of quantum-well structures on the thermoelectric figure of merit, Phys. Rev. B. 47 (1993) 12727–12730.

[5] Harman T.C., Spears D.L., Manfra M.J., High thermoelectric figures of merit in PbTe quantum wells, J. Electron. Mat. 25 (1996) 1121–1127.

[6] Berman R., Thermal Conduction in Solids, Oxford, Clarendon Press, 1976.

[7] Ziman J.M., Electrons and Phonons, Oxford, 1960.

[8] Hyldgaard P., Mahan G.D., Phonon Knudson flow in superlattices, in: Wilkes K.E., Dinwiddie R.B., Graves R.S. (Eds.), Thermal Conductivity, Vol. 23, 1995, pp. 172–182.

[9] Chen G., Size and interface effects on heat conduction in superlattices, J. Heat Tran. 119 (1997) 220–229.

[10] Chen G., Ballistic phonon transport in the cross-plane direction of superlattices, Phys. Rev. B 57 (1998) 14958–14973.

[11] Born M., Wolf E., Principles of Optics, 6th Edition, Pergamon, 1980, p. 491.

[12] Chen G., Tien C.L., Partial coherence theory of thin film radiative properties, J. Heat Tran. 114 (1992) 636–643.

[13] Kittel C., Introduction to Solid State Physics, 7th Edition, Wiley, 1996.

[14] Ashcroft N.W., Mermin N.D., Solid State Physics, Holt, Rinehart and Winston, 1976.

[15] Chen G., Wave effects on heat conduction of thin films and superlattices, J. Heat Tran. 121 (1999) 945–953.

[16] Tamura S., Hurley D.C., Wolfe J.P., Acoustic-phonon propagation in superlattices, Phys. Rev. B 38 (1989) 1427–1449.

[17] Colvard C., Gant T.A., Klein M.V., Merlin R., Fisher R., Morkoc H., Gossard A.C., Folded acoustic and quantized optic phonons in (GaAl)As superlattices, Phys. Rev. B 31 (1985) 2080–2091.

[18] Stroscio M.A., Kim K.W., Yu S.G., Ballato A., Quantized acoustic phonon modes in quantum wires and quantum dots, J. Appl. Phys. 76 (1994) 4670–4675.

[19] Balandin A., Wang K.L., A significant decrease of the lattice thermal conductivity due to phonon confinement in a free-standing semiconductor quantum well, Phys. Rev. B 58 (1998) 1544–1549.

[20] Hyldgaard P., Mahan G.D., Phonon superlattice transport, Phys. Rev. B. 56 (1997) 10754–10757.

[21] Chen G., Neagu M., Thermal conductivity and heat conduction in superlattices, Appl. Phys. Lett. 71 (1997) 2761–2764.

[22] Volz S., Chen G., Heat conduction in Si nanowires, Appl. Phys. Lett., submitted.

[23] Yao T., Thermal properties of AlAs/GaAs superlattices, Appl. Phys. Lett. 51 (1987) 1798–1800.

[24] Yu X.Y., Chen G., Verma A., Smith J.S., Temperature dependence of thermophysical properties of GaAs/AlAs periodic thin film structures, Appl. Phys. Lett. 67 (1995) 3553–3556, 68 (1995) 1303.

[25] Chen G., Hadley M.A., Smith J.S., Pulsed and continuous wave thermal characteristics of external-cavity surface-emitting laser diodes, J. Appl. Phys. 76 (1994) 3261–3271.

[26] Goldsmid H., Thermoelectric Refrigeration, Plenum Press, 1964.

[27] Yu X.Y., Zhang L., Chen G., Thermal-wave measurement of thin-film thermal diffusivity with different laser beam configurations, Rev. Sci. Instrum. 67 (1996) 2312–2316.

[28] Asheghi M., Leung Y.K., Wong S.S., Goodson K.E., Phonon-boundary scattering in thin silicon layers, Appl. Phys. Lett. 71 (1997) 1798–1800.

[29] Zheng X.Y., Li S.Z., Chen M., Wang K.L., Giant reduction in lateral thermal conductivity of thin nitride/silicon/oxide membrane measured with a micro thermal bridge, in: ASME DSC, Vol. 59, 1996, pp. 93–97.

[30] Little W.A., The transport of heat between dissimilar solids at low temperatures, Can. J. Phys. 37 (1959) 334–349.

[31] Lee S.-M., Cahill D.G., Venkatasubramanian R., Thermal conductivity of Si/Ge superlattices, Appl. Phys. Lett. 70 (1997) 2957–2959.

[32] Capinski W.S., Maris H.J., Thermal conductivity of GaAs/AlAs superlattices, Physica B 219 (1996) 699–701.

[33] Chen G., Zhou S., Yao D.-J., Kim C.J., Zheng X.Y., Liu J.-L., Wang K.L., Heat conduction in alloy-based superlattices, in: Proceedings of 17th International Thermoelectrics Conference, Nagoya, Japan, 1998, pp. 202–205.

[34] Chen G., Non-local heat conduction in the vicinity of nanoparticles, J. Heat Tran. 118 (1996) 539–545.

[35] Weisbuch C., Vinter B., Quantum Semiconductor Structures: Fundamentals and Applications, Academic Press, 1991.

[36] Yablonovitch E., Inhibited spontaneous emission in solid-state physics and electronics, Phys. Rev. Lett. 58 (1986) 2059–2062.

[37] Chen G., Tien C.L., Wu X., Smith J.S., Thermal diffusivity measurement of GaAs/AlGaAs thin-film structures, J. Heat Tran. 116 (1994) 325–331.

[38] Norris P.M., Chen G., Tien C.L., Size effects on the temperature rise in vertical-cavity surface emitting lasers, Int. J. Heat Mass Tran. 37 (1994) 9–17.

[39] Shakouri A., Bowers J., Heterostructure integrated thermionic coolers, Appl. Phys. Lett. 71 (1997) 1234–1236.

[40] Mahan G.D., Sofo J.O., Bartkowiak M., Multilayer thermionic refrigerator and generator, J. Appl. Phys. 83 (1998) 4683–4689.

[41] Sun X., Chen G., Wang K.L., Dresselhaus M.S., Theoretical modeling of the thermoelectric figure of merit in $Si/Si_{0.8}Ge_{0.2}$ quantum well structures, in: Proceedings of 17th International Thermoelectrics Conference, Nagoya, Japan, 1998, pp. 47–50.

[42] Chen G., Borca-Tasciuc T., Yang B., Song D., Liu W.L., Zeng T., Achimov D.-A., Heat conduction mechanisms and phonon engineering in superlattice structures, Thermal Science and Engineering 7 (1999) 43–51.